World Academy of Science, Engineering and Technology
International Journal of Energy and Power Engineering
Vol:12, No:9, 2018

Investigation on a Wave-Powered Electrical Generator Consisted of a Geared Motor-Generator Housed by a Double-Cone Rolling on Concentric Circular Rails

Barenten Suciu

Open Science Index, Energy and Power Engineering Vol:12, No:9, 2018 publications.waset.org/10009395.pdf

Abstract**—**An electrical generator able to harness energy from the water waves and designed as a double-cone geared motor-generator (DCGMG), is proposed and theoretically investigated. Similar to a differential gear mechanism, used in the transmission system of the auto vehicle wheels, an angular speed differential is created between the cones rolling on two concentric circular rails. Water wave acting on the floating DCGMG produces and a gear-box amplifies the speed differential to gain sufficient torque for power generation. A model that allows computation of the speed differential, torque, and power of the DCGMG is suggested. Influence of various parameters, regarding the construction of the DCGMG, as well as the contact between the double-cone and rails, on the electro-mechanical output, is emphasized. Results obtained indicate that the generated electrical power can be increased by augmenting the mass of the double-cone, the span of the rails, the apex angle of the cones, the friction between cones and rails, the amplification factor of the gear-box, and the efficiency of the motor-generator. Such findings are useful to formulate a design methodology for the proposed wave-powered generator.

Keywords**—**Wave-powered electrical generator, double-cone, circular concentric rails, amplification of angular speed differential.

I. Introduction

At global scale of the Earth, the electrical power generation from the energy of sea and ocean waves has same potential as the hydraulic and geothermal electric power generation [1], [2]. However, such huge source of alternative energy appears as under-developed, since the structural integrity of the devices proposed up to now cannot be guaranteed under the extreme loading conditions of heavy sea waves and tsunamis [3], [4].

Quite a large variety of systems for power generation from water waves are using buoys fixedly attached to rods, pendular buoys hinged to rods, and pendular buoys hinged between them [1]-[6]. Wave movement is converted either into the alternative translational motion of a bar, or into the rotational motion of a shaft coupled to a dynamo. By employing a suitable mechanism, the reciprocating motion of the bar can be further transformed into the rotational motion of a shaft. On the other hand, electricity can be directly obtained from the reciprocating motion of the bar by using inductive, piezoelectric or dielectric devices.

As alternative to buoyant generators, gyroscopic [7]-[10] and double-cone [11] power generators were proposed. On one hand, waves rotate the floater of the gyroscope, and this rotational motion is transmitted to the gyroscopic precession axis that is linked to the shaft of a dynamo [10]. On the other hand, in the case of the previously suggested double-cone generators [11], the rotational motion of the buoy, is changed into the rotational and translational motion of a magnetized double-cone, which is rolling on divergent-convergent rails, materialized by using either straight V-rails or eccentric circular rails Movable magnetic double-cone extends a fluctuating field across the electrical conductors wound inside the rails, electricity being achieved via electromagnetic induction [11].

In this paper, a different wave-powered electrical generator, using a DCGMG that runs on two circular concentric rails is investigated. In the case of the proposed device, instead of employing a double-cone consisted of two rigidly coupled cones [11]-[16], relative rotation between cones is allowed by using a geared motor- generator. Similar to a classical differential gear [17], [18], an angular speed difference between cones can be produced and multiplied by the gear-box of the motor-generator. Purpose of this study is to clarify the effect of different geometrical and tribological parameters on the power output of the DCGMG.

II. Description of the Proposed DCGMG

DCGMG consists of a geared motor-generator, housed by a double-cone, which is travelling on two concentric circular rails, of outer radius R_o, and inner radius R_i (Figs. 1 and 2).

Classical rigid double-cone [11]-[16], composed of two fixedly joined cones, is replaced by a double-cone where the relative rotation motion between the inner and outer cones is permitted by a rotational-link, i.e. by a geared motor-generator. In a possible design of the DCGMG, inner cone accommodates the casing of the motor-generator, and its shaft is press-fitted into the outer cone, along the axis of symmetry of the DCGMG assembly. Inner and outer cones have the same height H, base radius R, and apex angle $\Psi = \tan^{-1}(R/H)$. Since a space of thickness t is provided between cones, the total height of the DCGMG becomes $H_t = 2H + t$ (Figs. 1, 2). Similar to differential gears, used in the transmission of autovehicle wheels, the outer cone is running along the longer outer rail, and hence, it rotates faster than the inner cone, which is running along the shorter inner rail. Such difference of angular speed between the inner and outer cones is amplified by the gear-box of the motor-generator. Hence, enough difference of angular

Barenten Suciu is with the Department of Intelligent Mechanical Engineering, Fukuoka Institute of Technology, Fukuoka, 811-0295 Japan (phone: +81-92-606-4348; fax: +81-92-606-0747; e-mail: suciu@fit.ac.jp).

Open Science Index, Energy and Power Engineering Vol:12, No:9, 2018 publications.waset.org/10009395.pdf

speed between stator and rotor is obtained to gain electrical power generation.

Movement of the DCGMG is attenuated by the inherent friction between the cones and the rails, but it can be sustained if wave energy is supplied from time to time into the system. Thus, waves of random direction, height and period are able to produce random rotation of the buoy, and implicitly of the rails. Quite small inclination angles of the tracks are sufficient to sustain the motion of revolution of the DCGMG around the rails, and to produce the angular speed differential between the inner and outer cones. Besides, full revolution of the DCGMG around the center of the rails is not a mandatory condition to achieve electrical power generation.

Table I shows the nomenclature associated to the proposed DCGMG.

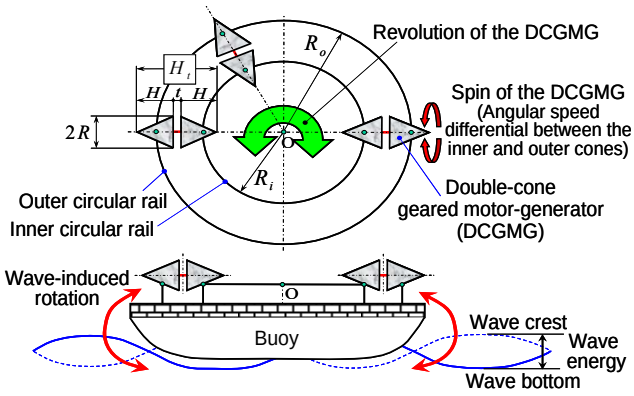

Fig. 1 Schematic view of the proposed wave-powered electrical generator consisted of a DCGMG running on two circular concentric rails

TABLE I
NOMENCLATURE ASSOCIATED TO THE PROPOSED DCGMG ASSEMBLY

Property	Notation and units
Base diameter of the inner and outer cones	$2R$ [mm]
Total height (length) of the DCGMG	H_t [mm]
Height of the inner and outer cones	H [mm]
Apex angle of the inner and outer cone	Ψ [deg]
Thickness of the space between the cones	t [mm]
Total mass of the DCGMG	m [g]
Mass of the outer cone	m_o [g]
Mass of the inner cone	m_i [g]
Moment of inertia of the outer cone	I_o [kg·mm^2]
Moment of inertia of the inner cone	I_i [kg·mm^2]
Outer radius of the rails	R_o [mm]
Inner radius of the rails	R_i [mm]
Dynamic sliding friction coefficient at the contact of the inner cone with the inner rail	μ_i [-]
Dynamic sliding friction coefficient at the contact of the outer cone with the outer rail	μ_o [-]
Moment of inertia of the shaft and rotor of the geared motor-generator	I_s [kg·mm^2]

III. THEORETICAL MODEL: CONTACT RADIUS AND THE ANGULAR SPEED DIFFERENTIAL OF THE DCGMG

Tangential speeds, corresponding to the contact points P and Q of the DCGMG with the inner and outer circular rails, can be written as (see Fig. 2):

$$\begin{cases} V_P = R_i\Omega = a_i\omega_i \\ V_Q = R_o\Omega = a_o\omega_o \end{cases} \quad (1)$$

where a_i is the contact radius of the inner cone with the inner rail, a_o is the contact radius of the outer cone with the outer rail, ω_i is the angular speed of the inner cone, ω_o is the angular speed of the outer cone, and Ω is the revolution speed of the DCGMG around the center O of the rails.

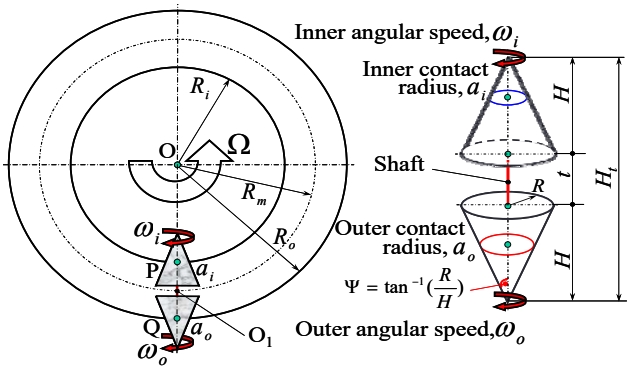

Fig. 2 Geometrical and kinematical parameters describing the contact of the DCGMG with the circular concentric rails

On the other hand, a geometrical relationship connecting the height of the DCGMG, the span of the rails, and the contact radii, can be obtained as follows (see Fig. 2):

$$H_t = 2H + t = R_o - R_i + \frac{a_i + a_o}{\tan\Psi} \quad (2)$$

Theoretical model will be developed under the assumption that the inner contact radius equals the outer contact radius:

$$a_i = a_o = a \quad (3)$$

Condition (3) is similar to the working condition of differential gears used in transmission system of the autovehicle wheels, in which the left and right tires have the same contact radius with the road. Besides, such condition can be easily achieved from a practical standpoint, for concentric circular rails, where the span of the tracks $R_o - R_i$ is constant. Under the imposed running condition (3), the contact radius of DCGMG with the rails can be written as:

$$a = 0.5R_o(\overline{H}_t + \overline{R}_i - 1)\tan\Psi \quad (4)$$

where $\overline{H}_t$ is the dimensionless height of the DCGMG, and $\overline{R}_i$ is the dimensionless radius of the inner rail, defined as:

$$\overline{H}_t = \frac{H_t}{R_o} = \frac{2H + t}{R_o} \quad ; \quad \overline{R}_i = \frac{R_i}{R_o} \quad (5)$$

Open Science Index, Energy and Power Engineering Vol:12, No:9, 2018 publications.waset.org/10009395.pdf

Since the span of the rails $R_o - R_i$ should be smaller than the height H_t of the DCGMG ($R_o - R_i \le H_t$), and since the inner radius R_i should be smaller than the outer radius R_o of the rails ($R_i \le R_o$), the following inequality can be obtained for the dimensionless radius of the inner rail:

$$1 - \overline{H}_t \le \overline{R}_i \le 1 \tag{6}$$

Next, from (1) in connection with (3) and (4), the angular speeds of the outer and inner cones can be derived as:

$$\begin{cases} \omega_o = \Omega \dfrac{R_o}{a_o} = \Omega \dfrac{R_o}{a} = \dfrac{2\Omega}{(\overline{H}_t + \overline{R}_i - 1)\tan\Psi} \\ \omega_i = \Omega \dfrac{R_i}{a_i} = \Omega \dfrac{R_i}{a} = \dfrac{2\Omega \overline{R}_i}{(\overline{H}_t + \overline{R}_i - 1)\tan\Psi} < \omega_o \end{cases} \tag{7}$$

Results (7) agree with the intuitive kinematics of the DCGMG, i.e. outer cone, which is running along the longer outer rail, rotates faster than inner cone, which is running along the shorter inner rail. Therefore, the difference of angular speed between the inner and outer cones can be written as:

$$\Delta\omega = \omega_o - \omega_i = \frac{2\Omega(1 - \overline{R}_i)}{(\overline{H}_t + \overline{R}_i - 1)\tan\Psi} \tag{8}$$

In order to completely describe the angular speed differential, the revolution speed Ω of the DCGMG around the center O of the rails should be determined, as shown in the next section.

IV. Theoretical Model: Contact Forces and the Revolution Speed of the DCGMG

In order to find the contact forces, i.e. the normal forces ($\vec{N}_Q$ and $\vec{N}_P$) as well as the frictional forces ($\vec{F}_{f,Q}$ and $\vec{F}_{f,P}$), acting in the contact points P and Q, and then, in order to obtain the revolution speed Ω of the DCGMG around the center O of the rails, the Newton's Law of Dynamics, concerning the mass center O_1 of the DCGMG, can be written as (see Fig. 3):

$$-mg\vec{k} + m\Omega^2 R_m \vec{j} + \vec{N}_Q + \vec{F}_{f,Q} + \vec{N}_P + \vec{F}_{f,P} = \vec{0} \tag{9}$$

Note that $\vec{F}_{f,Q}$ and $\vec{F}_{f,P}$ are sliding friction forces, taken along the conical generatrices, and they can be calculated as:

$$F_{f,Q} = \mu_o N_Q \quad ; \quad F_{f,P} = \mu_i N_P \tag{10}$$

where μ_o is the sliding friction coefficient at the contact of the outer cone with the outer rail, and μ_i is the sliding friction coefficient at the contact of the inner cone with the inner rail.

On the other hand, $-mg\vec{k}$ is the force of gravity, and $m\Omega^2 R_m \vec{j}$ is the centrifugal force acting on the DCGMG, where the mean radius of the rails is given by (see Fig. 2):

$$R_m = \frac{R_o + R_i}{2} = \frac{R_o}{2}(1 + \overline{R}_i) \tag{11}$$

Next, projection of (9) along the axes O_1y and O_1z leads to:

$$\begin{cases} 0.5m\Omega^2 R_0 (1 + \overline{R}_i) = \\ \quad = N_Q(\sin\Psi + \mu_o \cos\Psi) - N_P(\sin\Psi - \mu_i \cos\Psi) \\ mg = N_Q(\cos\Psi - \mu_o \sin\Psi) + N_P(\cos\Psi + \mu_i \sin\Psi) \end{cases} \tag{12}$$

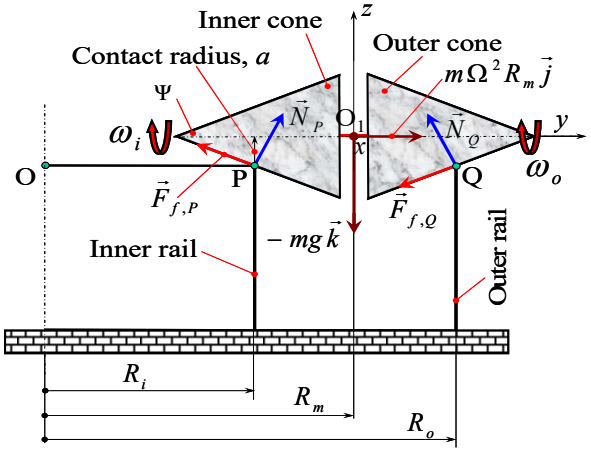

Fig. 3 Equilibrium of forces and moments acting on the DCGMG

Since (12) gives a set of two equations with three unknowns (Ω, N_Q, N_P), in order to completely solve the problem, a third equation should be added. For instance, in an approximate but simplified approach, one might assume that the normal force at the inner contact point P equals the normal force at the outer contact point Q ($N_Q \cong N_P$). In such conditions, (12) leads to the following approximate contact forces:

$$N_{Q,a} = N_{P,a} = \frac{mg}{\cos\Psi} \frac{1}{2 - (\mu_o - \mu_i)\tan\Psi} \tag{13}$$

and, the approximate revolution speed of the DCGMG, around the center O of the rails:

$$\Omega_a^2 = \frac{2g}{R_o(1 + \overline{R}_i)} \frac{\mu_o + \mu_i}{2 - (\mu_o - \mu_i)\tan\Psi} \tag{14}$$

However, a correct approach of the problem requires the addition of the equilibrium equation at rotation of the DCGMG around the axis O_1x (see Fig. 3). Since the gravitational and centrifugal forces pass through the point O_1, their moments are nil. Consequently, the rotational equilibrium is dictated by the moments corresponding to the normal and frictional forces, leading to the following relationship between N_Q and N_P:

$$N_Q \cdot f_1 = N_P \cdot f_2 \tag{15}$$

where the functions f_1 and f_2 of (15) can be defined as:

$$\begin{cases} f_1 = 1 - \overline{R}_i - \overline{H}_t\left(1 + \dfrac{\mu_o}{\tan\Psi}\right)\sin^2\Psi \\ f_2 = 1 - \overline{R}_i - \overline{H}_t\left(1 - \dfrac{\mu_i}{\tan\Psi}\right)\sin^2\Psi \end{cases} \tag{16}$$

In such circumstances, (12) in correlation with (15)-(16) leads to the following exact contact forces:

$$\begin{cases} N_Q = \dfrac{mg \cdot f_2}{(\cos\Psi - \mu_o \sin\Psi) f_2 + (\cos\Psi + \mu_i \sin\Psi) f_1} \\ N_P = \dfrac{mg \cdot f_1}{(\cos\Psi - \mu_o \sin\Psi) f_2 + (\cos\Psi + \mu_i \sin\Psi) f_1} \end{cases} \tag{17}$$

and, the exact revolution speed of the DCGMG, around the center O of the rails:

$$\Omega^2 = \frac{2g}{R_o(1+\overline{R}_i)} \times \\ \times \frac{(\sin\Psi + \mu_o \cos\Psi) f_2 - (\sin\Psi - \mu_i \cos\Psi) f_1}{(\cos\Psi - \mu_o \sin\Psi) f_2 + (\cos\Psi + \mu_i \sin\Psi) f_1} \tag{18}$$

On one hand, one observes that:

$$f_2 - f_1 = \overline{H}_t(\mu_o + \mu_i)\sin\Psi\cos\Psi > 0 \quad \Rightarrow \quad f_2 > f_1 \tag{19}$$

which leads to the conclusion that the outer contact force N_Q is larger than the inner contact force N_P, a result consistent with equilibrium of moments on the DCGMG (see Fig. 3).

On the other hand, after some manipulations, (18) can be rewritten as:

$$\Omega^2 = \frac{2g}{R_o(1+\overline{R}_i)} \frac{\mu_o + \mu_i}{2 - (\mu_o - \mu_i)\tan\Psi - \overline{H}_t C/(1-\overline{R}_i)} \tag{20}$$

where the constant C can be calculated as:

$$C = \sqrt{(1+\mu_o^2)(1+\mu_i^2)}\,\tan\Psi \cdot \sin(2\Psi + \rho_o - \rho_i) \tag{21}$$

in which ρ_o and ρ_i are the friction angles, given by:

$$\rho_o = \tan^{-1}(\mu_o) \quad ; \quad \rho_i = \tan^{-1}(\mu_i) \tag{22}$$

Note that the more complex but exact solutions for contact forces and revolution speed, given by (17) and (20), resemble somewhat the approximate but simpler solutions, given by (13)-(14). However, the usage of (17) and (20) in the analytical and numerical calculations becomes less convenient.

Additionally, since $\Omega^2 \geq 0$, from (20) combined with (21), one obtains a new restrictive condition on the dimensionless radius of the inner rail, which comes to replace the right part of the inequality (6), as follows:

$$\overline{R}_i \leq 1 - \overline{H}_t \frac{C}{2 - (\mu_o - \mu_i)\tan\Psi} = 1 - \overline{H}_t \overline{C} \tag{23}$$

in which $\overline{C}$ denotes the ratio $C/[2 - (\mu_o - \mu_i)\tan\Psi]$.

V. Theoretical Model: Torque and Power at the Shaft of the DCGMG

In order to determine the torque acting on the shaft of the DCGMG, one should take into account the equation of dynamic equilibrium at rotation around the axis O_1y, for the outer cone (see Fig. 4), and also for the inner cone (see Fig. 5).

Firstly, Fig. 4 leads to the following equation of rotational dynamic equilibrium:

$$I_o \varepsilon_o = aF_{f,o} - M_t \tag{24}$$

where I_o is the moment of inertia of the outer cone (see Table I), ε_o is the angular acceleration of the outer cone, a is the radius of contact given by (4), $F_{f,o}$ is the rolling friction force acting on the outer cone, and M_t is the torque acting on the shaft of the DCGMG.

On the other hand, Fig. 5 leads to the following set of equations of dynamic equilibrium, one equation being for the rotation of the inner cone, and the other for the rotor of the motor-generator, which is housed inside the inner cone:

$$\begin{cases} I_i \varepsilon_i = M_r + aF_{f,i} \\ I_s \varepsilon_s = M_t - M_r \end{cases} \tag{25}$$

where I_i is the moment of inertia of the inner cone (Table I), I_s is the moment of inertia of the shaft-rotor assembly of the motor-generator (Table I), ε_i is the angular acceleration of the inner cone, ε_s is the angular acceleration of the shaft-rotor assembly of the motor-generator, $F_{f,i}$ is the rolling friction force acting on the inner cone, and M_r is the resistant electro-magnetic torque occurring between the rotor and stator.

Additionally, the angular speeds and accelerations satisfy the following relationships (see the DCGMG construction and (7)):

$$\begin{cases} \omega_i = \omega_o \overline{R}_i \quad \Rightarrow \quad \varepsilon_i = \varepsilon_o \overline{R}_i \\ \omega_s = \omega_o \quad \Rightarrow \quad \varepsilon_s = \varepsilon_o \end{cases} \tag{26}$$

Combining (24)-(26), one finds after several manipulations the following expression for the torque acting on the shaft of the DCGMG:

Open Science Index, Energy and Power Engineering Vol:12, No:9, 2018 publications.waset.org/10009395.pdf

$$M_t = a\frac{(I_s + I_i\overline{R}_i)F_{f,o} - I_oF_{f,i}}{I_o + I_s + I_i\overline{R}_i} \quad (27)$$

It can be argued that ratio of the moments of inertia satisfies the following relations:

$$\frac{I_s}{I_o} \cong 0 \quad ; \quad \frac{I_i}{I_o} \cong 1 \quad (28)$$

and in such conditions, torque at the shaft of the DCGMG can be approximately, but quite accurately, calculated as:

$$M_t \cong -a\frac{F_{f,i} - \overline{R}_iF_{f,o}}{1 + \overline{R}_i} \quad (29)$$

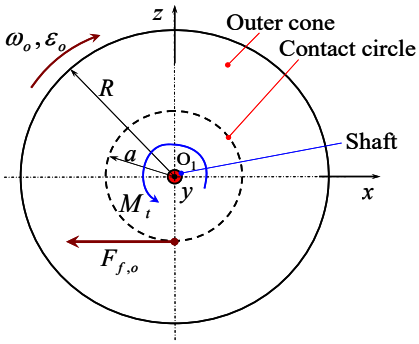

Fig. 4 Equilibrium of moments on the outer cone around O_1y axis

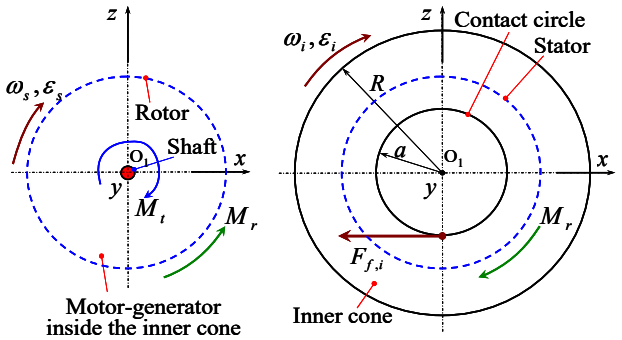

Fig. 5 Equilibrium of moments on the shaft-rotor assembly, and on the stator-inner cone assembly, around the O_1y axis

In order to completely determine the torque, one should add the equation of equilibrium at rotation around the axis O_1z of the DCGMC (see Fig. 6), as follows:

$$F_{f,o}(R_o - R_m) = F_{f,i}(R_m - R_i) \quad (30)$$

Since the arms of frictional forces $F_{f,o}$ and $F_{f,i}$, are identical:

$$R_o - R_m = R_m - R_i = 0.5R_o(1 - \overline{R}_i) \quad (31)$$

equality of the rolling friction forces is implicitly achieved:

$$F_{f,o} = F_{f,i} \quad (32)$$

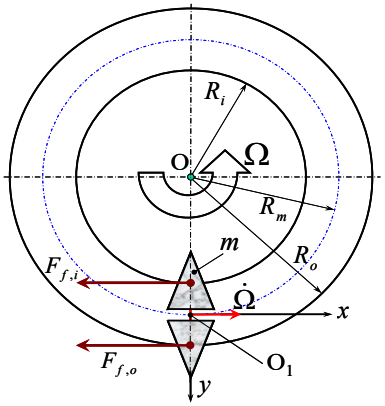

Fig. 6 Equilibrium at rotation of the DCGMG around the O_1z axis, and the Newton's Law of Dynamics applied to the mass center O_1, along the O_1x axis

Next, the Newton's Law of Dynamics, applied to the mass center O_1 of the DCGMG, along the O_1x axis can be written as:

$$-F_{f,o} - F_{f,i} = mR_m\dot{\Omega} = 0.5mR_o(1 + \overline{R}_i)\dot{\Omega} \quad (33)$$

where $\dot{\Omega}$ is the angular acceleration at the revolution of the DCGMG, around the center O of the circular rails (see Fig. 6).

Substituting in (29) the contact radius a as given by (4), and the results (32)-(33), one obtains the following expression for the torque acting on the shaft of the DCGMG:

$$M_t = 0.125mR_o^2(1 - \overline{R}_i)(\overline{H}_t + \overline{R}_i - 1)\dot{\Omega}\tan\Psi \quad (34)$$

Taking the angular acceleration $\dot{\Omega}$ for the movement of revolution of the DCGMG around the center of the rails, as the ratio of the angular speed Ω to the wave period T (Fig. 7):

$$\dot{\Omega} = \Omega / T \quad (35)$$

torque acting on the shaft of the motor-generator becomes:

$$M_t = \frac{mR_o^2}{8T}(1 - \overline{R}_i)(\overline{H}_t + \overline{R}_i - 1)\Omega\tan\Psi \quad (36)$$

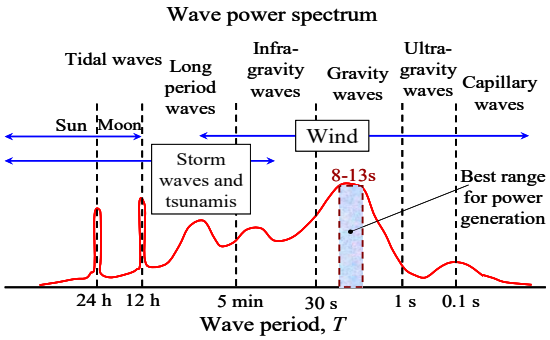

Fig. 7 Sea and ocean wave spectrum

Open Science Index, Energy and Power Engineering Vol:12, No:9, 2018 publications.waset.org/10009395.pdf

Open Science Index, Energy and Power Engineering Vol:12, No:9, 2018 publications.waset.org/10009395.pdf

While the best range of wave period for power generation is $T = 8\text{-}13$ s (see Fig. 7), the angular speed Ω can be substituted in (36) from (14), leading to an approximate expression for the torque computation:

$$M_{t,a} = \sqrt{\frac{m^2 R_o^3 g(\mu_o + \mu_i)\tan^2\Psi}{32T^2}} \times \times \sqrt{\frac{(1-\overline{R}_i)^2(\overline{H}_t + \overline{R}_i - 1)^2}{[2-(\mu_o - \mu_i)\tan\Psi](1+\overline{R}_i)}} \tag{37}$$

or from (20), giving an exact formula for the torque calculus:

$$M_t = \sqrt{\frac{m^2 R_o^3 g(\mu_o + \mu_i)\tan^2\Psi}{32T^2}} \times \times \sqrt{\frac{(1-\overline{R}_i)^3(\overline{H}_t + \overline{R}_i - 1)^2}{[2-(\mu_o - \mu_i)\tan\Psi](1-\overline{R}_i^2) - \overline{H}_t C(1+\overline{R}_i)}} \tag{38}$$

Then, the mechanical power inputted at the shaft of the motor-generator used in the construction of the DCGMG, and the electrical power outputted by DCGMG can be calculated as:

$$P_{mech} = M_t \cdot \Delta\omega \quad ; \quad P_{el} = \eta \cdot P_{mech} \tag{39}$$

where η is the efficiency of the motor-generator [19]-[21].

Substituting in (39) the torque (36), and the angular speed differential $\Delta\omega$ as given by (8), the mechanical power can be rewritten as:

$$P_{mech} = \frac{mR_o^2}{4T}(1-\overline{R}_i)^2\Omega^2 \tag{40}$$

Term Ω^2 can be substituted in (40) from (14), leading to the following approximate expression for the calculus of the mechanical power:

$$P_{mech,a} = \frac{mgR_o}{2T(1+\overline{R}_i)} \frac{(\mu_o + \mu_i)(1-\overline{R}_i)^2}{2-(\mu_o - \mu_i)\tan\Psi} \tag{41}$$

or from (20), furnishing the next exact formula of computation for the mechanical power:

$$P_{mech} = \frac{mgR_o}{2T(1+\overline{R}_i)} \frac{(\mu_o + \mu_i)(1-\overline{R}_i)^3}{[2-(\mu_o - \mu_i)\tan\Psi](1-\overline{R}_i) - \overline{H}_t C} \tag{42}$$

VI. Results and Discussions

Fig. 8 shows, based on (4)-(6) and (23), the linear ascending variation of the dimensionless radius of contact $\overline{a} = a/R_o$ versus the dimensionless radius $\overline{R}_i$ of the inner rail. As expected, radius of contact decreases at augmentation of the dimensionless span $1-\overline{R}_i$ of the rails.

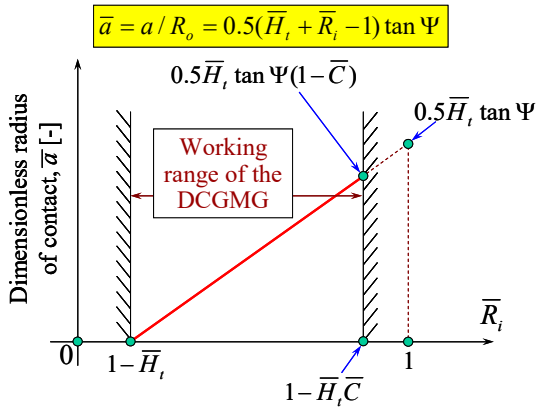

Fig. 8 Variation of the dimensionless radius of contact versus the dimensionless radius of the inner rail

Concerning the parameter $\overline{C} = C/[2-(\mu_o - \mu_i)\tan\Psi]$ that occurs in the description of the results presented by Figs. 8-21, three distinct cases can be taken into account (see (21)-(22)). Concretely, regarding the magnitude of the friction coefficient μ_o at the contact of the outer cone with the outer rail, relative to the friction coefficient μ_i at the contact of the inner cone with the inner rail, three distinct cases can be defined as:

$$\begin{cases} \mu_o >> \mu_i \;\Rightarrow\; \overline{C} \cong \dfrac{\tan\Psi\sin(2\Psi + \rho_o)}{2\cos\rho_o - \tan\Psi\sin\rho_o} \\ \mu_o \cong \mu_i \;\Rightarrow\; \overline{C} \cong \dfrac{\sin^2\Psi}{\cos^2\rho_o} \\ \mu_o << \mu_i \;\Rightarrow\; \overline{C} \cong \dfrac{\tan\Psi\sin(2\Psi - \rho_i)}{2\cos\rho_i + \tan\Psi\sin\rho_i} \end{cases} \tag{43}$$

Next, Fig. 9 shows based on (14) the nonlinear descending variation of the dimensionless approximate revolution speed $\overline{\Omega}_a$ of the DCGMG versus the dimensionless radius $\overline{R}_i$ of the inner rail.

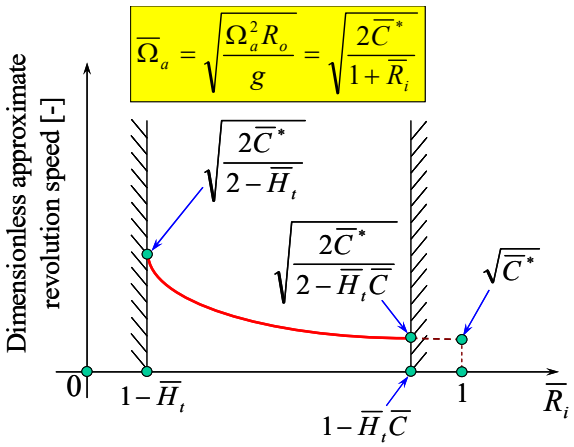

Fig. 9 Variation of the dimensionless approximate revolution speed of the DCGMG versus the dimensionless radius of the inner rail

Open Science Index, Energy and Power Engineering Vol:12, No:9, 2018 publications.waset.org/10009395.pdf

It is useful to observe that, similar to (43), for the parameter $\overline{C}^* = (\mu_o + \mu_i)/[2-(\mu_o - \mu_i)\tan\Psi]$, which occurs on Figs. 9-21, three distinct cases can be taken into account, as follows:

$$\begin{cases} \mu_o >> \mu_i \quad \Rightarrow \quad \overline{C}^* \cong \dfrac{\tan\rho_o}{2-\tan\Psi\tan\rho_o} = \dfrac{\mu_o}{2-\mu_o\tan\Psi} \\ \mu_o \cong \mu_i \quad \Rightarrow \quad \overline{C}^* \cong \tan\rho_o = \mu_o \\ \mu_o << \mu_i \quad \Rightarrow \quad \overline{C}^* \cong \dfrac{\tan\rho_i}{2+\tan\Psi\tan\rho_i} = \dfrac{\mu_i}{2+\mu_i\tan\Psi} \end{cases} \tag{44}$$

Next, Fig. 10 shows, based on (20), the valley-like variation of the dimensionless exact revolution speed $\overline{\Omega}$ of the DCGMG versus the dimensionless radius $\overline{R}_i$ of the inner rail, obtained under the condition $\overline{C} < \overline{H}_t/2$. Compared to the approximate speed $\overline{\Omega}_a$, the exact speed $\overline{\Omega}$ shows a different pattern of variation against the radius of the inner rail. Thus, $\overline{\Omega}$ tends to infinity for $\overline{R}_i \to 1-\overline{H}_t\overline{C}$, and displays a minimum for $\overline{R}_i = 1-\sqrt{2\overline{H}_t\overline{C}}$. On the other hand, Fig. 11 shows, based on (20), the nonlinear ascending variation of the dimensionless exact revolution speed $\overline{\Omega}$ of the DCGMG versus the dimensionless radius $\overline{R}_i$ of the inner rail, obtained under the condition $\overline{C} \geq \overline{H}_t/2$, i.e. under the following restriction:

$$\mu_o \geq \frac{\mu_i\tan\Psi(\cos 2\Psi + 0.5\overline{H}_t) + \overline{H}_t - \tan\Psi\sin 2\Psi}{\tan\Psi(\mu_i\sin 2\Psi + 0.5\overline{H}_t + \cos 2\Psi)} \tag{45}$$

Fig. 12 compares the results separately presented by Figs. 9-11, concerning the revolution speed of the DCGMG, obtained using the approximate solution (14), and the exact solution (20), for both conditions $\overline{C} < \overline{H}_t/2$ and $\overline{C} \geq \overline{H}_t/2$.

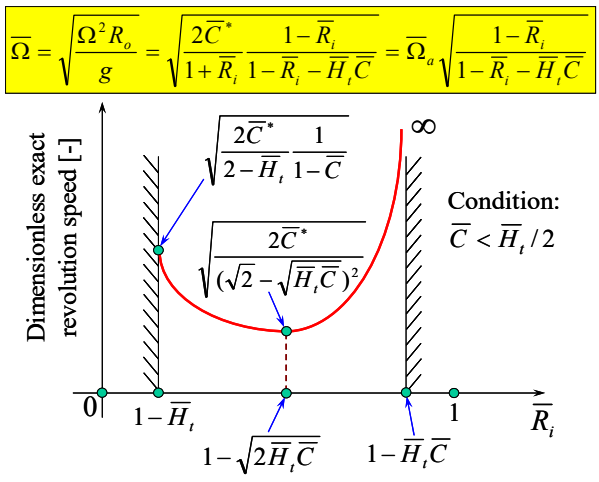

Fig. 10 Variation of the dimensionless exact revolution speed of the DCGMG versus the dimensionless radius of the inner rail, obtained under the condition: $\overline{C} < \overline{H}_t/2$

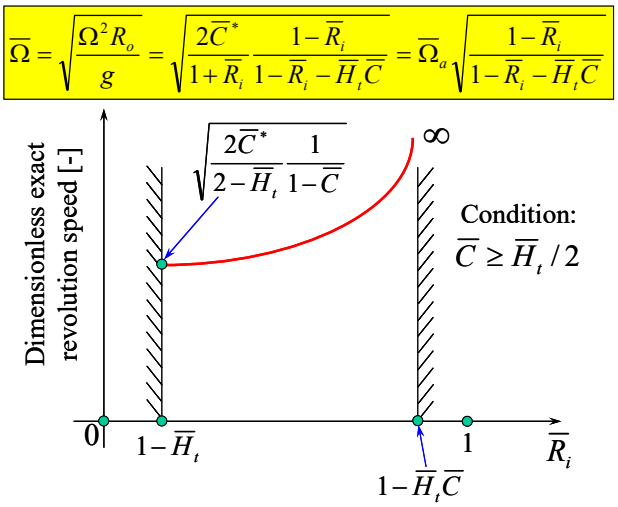

Fig. 11 Variation of the dimensionless exact revolution speed of the DCGMG versus the dimensionless radius of the inner rail, obtained under the condition: $\overline{C} \geq \overline{H}_t/2$

One observes that the approximate speed $\overline{\Omega}_a$ appears to be smaller than the exact speed $\overline{\Omega}$, and the augmentation of $\overline{C}$, i.e. the augmentation of the friction at the outer cone (see (45)) is beneficial for the amplification of the revolution speed. In conclusion, despite the complexity of analytical and numerical calculus, design of the water wave-powered generator should be performed based on the exact expression for the revolution speed of the DCGMG.

Fig. 13 shows, based on (8) combined with (14), the non-linear descending variation of the approximate difference of angular speed $\Delta\omega_a$ between the outer and inner cones of the DCGMG versus the dimensionless radius $\overline{R}_i$ of the inner rail.

On the other hand, Fig. 14 shows, based on (8) combined with (20), the valley-like variation of the exact difference of angular speed $\Delta\omega$ between the outer and inner cones of the DCGMG versus the dimensionless radius $\overline{R}_i$ of the inner rail.

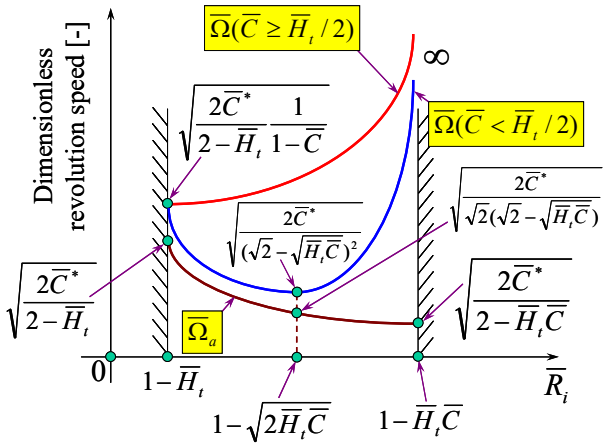

Fig. 12 Comparison of the results concerning the variation of the dimensionless revolution speed of the DCGMG versus the dimensionless radius of the inner rail

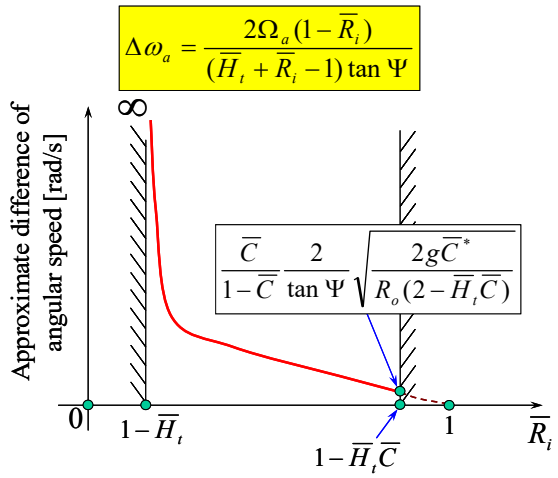

Fig. 13 Variation of the approximate difference of angular speed between the outer and inner cones of the DCGMG versus the dimensionless radius of the inner rail

Exact difference of angular speed $\Delta\omega$ displays a minimum for $\overline{R}_i = 1-3\overline{H}_t\overline{C}/(2+\overline{C})$:

$$\Delta\omega_{\min} = \frac{\overline{C}}{1-\overline{C}}\frac{3}{\tan\Psi}\sqrt{\frac{3g\overline{C}^*(2+\overline{C})}{R_o(1-\overline{C})(2+\overline{C}-1.5\overline{H}_t\overline{C})}} \tag{46}$$

and tends to infinity for $\overline{R}_i \to 1-\overline{H}_t$ and for $\overline{R}_i \to 1-\overline{H}_t\overline{C}$.

Fig. 15 compares the results separately presented by Figs. 13 and 14, concerning the difference of angular speed between the outer and inner cones of the DCGMG obtained by using the approximate and exact solutions. As expected, the approximate difference of angular speed $\Delta\omega_a$ has a different pattern of variation against the radius of the inner rail, and it is smaller than the exact difference of angular speed $\Delta\omega$ for any R_i.

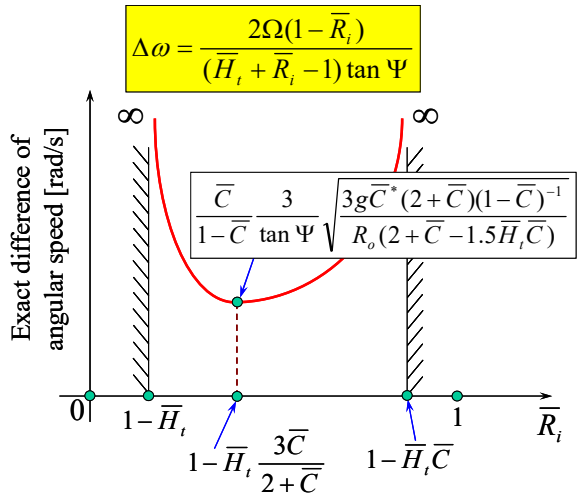

Fig. 14 Variation of the exact difference of angular speed between the outer and inner cones of the DCGMG versus the dimensionless radius of the inner rail

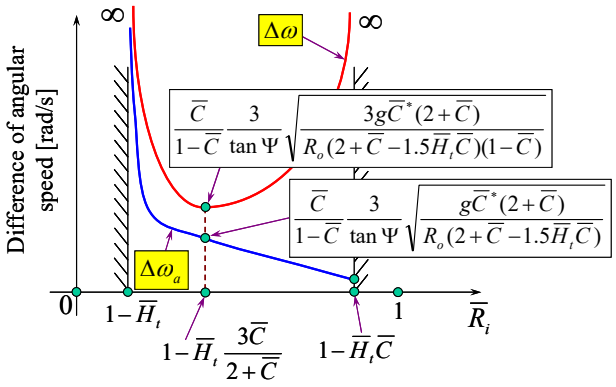

Fig. 15 Comparison of the results concerning the variation of the difference of angular speed between the outer and inner cones of the DCGMG versus the dimensionless radius of the inner rail

Next, by imposing in (8) the condition $\Omega = 1$, i.e. during one complete revolution of the DCGMG around the center O of the rails, the differential of the number of rotations between the outer and inner cones, can be written as:

$$\Delta N = N_o - N_i = \frac{2(1-\overline{R}_i)}{(\overline{H}_t+\overline{R}_i-1)\tan\Psi} \tag{47}$$

Accordingly, the differential ΔN decreases at augmentation of the dimensionless radius $\overline{R}_i$ of the inner rail.

Fig. 16 shows, based on (37), the mountain-like variation of the dimensionless approximate torque $\overline{M}_{t,a} = M_{t,a}/M_{t,0}$ at the shaft of the geared motor-generator versus the dimensionless radius $\overline{R}_i$ of the inner rail, where the referential torque $M_{t,0}$ is defined as follows:

$$M_{t,0} = \frac{mR_o}{4T}\overline{H}_t^2\sqrt{R_o g}\tan\Psi \tag{48}$$

Thus, torque $\overline{M}_{t,a}$ displays a maximum for $\overline{R}_i = 1-\overline{H}_t/3$, and becomes nil for $\overline{R}_i = 1-\overline{H}_t$, as well as for $\overline{R}_i = 1$.

Fig. 17 shows, based on (38), the nonlinear variation of the dimensionless exact torque $\overline{M}_t = M_t/M_{t,0}$ at the shaft of the geared motor-generator versus the dimensionless radius $\overline{R}_i$ of the inner rail. Note that the torque $\overline{M}_t$ starts from a nil value at $\overline{R}_i = 1-\overline{H}_t$, displays a maximum for $\overline{R}_i = 1-2\overline{H}_t\overline{C}$, as well as a minimum for $\overline{R}_i = 1-\overline{H}_t/3$, and finally tends to infinity for $\overline{R}_i \to 1-\overline{H}_t\overline{C}$. Such torque distribution is obtained under the condition that the point corresponding to the maximal value of the torque ($\overline{R}_i = 1-2\overline{H}_t\overline{C}$) exceeds $\overline{R}_i = 1-\overline{H}_t$, i.e. under the condition $\overline{C} < 1/2$. Moreover, minimal value of the torque can be reached only under the condition that the square root exists, i.e. under the restriction $\overline{C} < 1/3$. In order to fulfill such condition, the following inequality, concerning the friction coefficient at the contact between the outer cone and the outer

Open Science Index, Energy and Power Engineering Vol:12, No:9, 2018 publications.waset.org/10009395.pdf

rail, should be satisfied:

$$\mu_o < \frac{2-3\tan\Psi\sin 2\Psi+\mu_i\tan\Psi(1+3\cos 2\Psi)}{\tan\Psi(1+3\cos 2\Psi+3\mu_i\sin 2\Psi)} \quad (49)$$

Thus, (45) and (49) determine the range in which the friction coefficient μ_o of the outer contact can be selected for a given friction coefficient μ_i of the inner contact, and for a given geometry of the wave-powered generator.

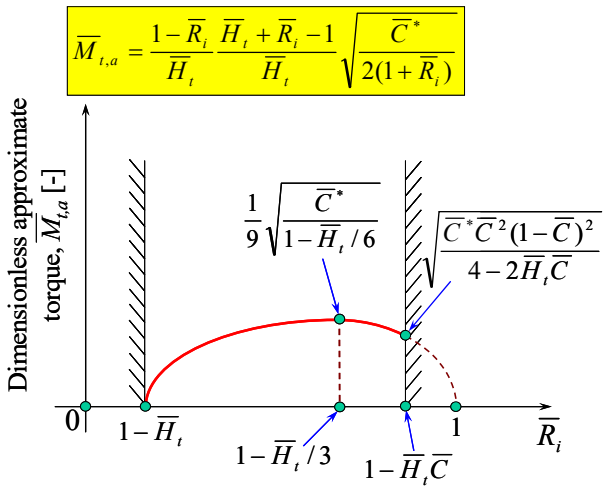

Fig. 16 Variation of the dimensionless approximate torque at the shaft of the motor-generator versus the dimensionless radius of the inner rail

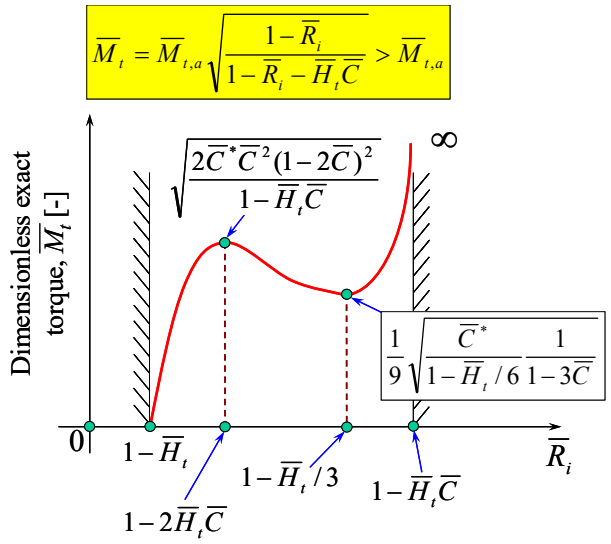

Fig. 17 Variation of the dimensionless exact torque at the shaft of the motor-generator versus the dimensionless radius of the inner rail

Fig. 18 compares the results separately presented by Figs. 16 and 17, concerning the dimensionless torque at the shaft of the DCGMG, found by using the approximate and exact solutions. As expected, the approximate torque $\overline{M}_{t,a}$ has a different pattern of variation against the radius of the inner rail, and it is smaller than the torque $\overline{M}_t$ for any $\overline{R}_i$.

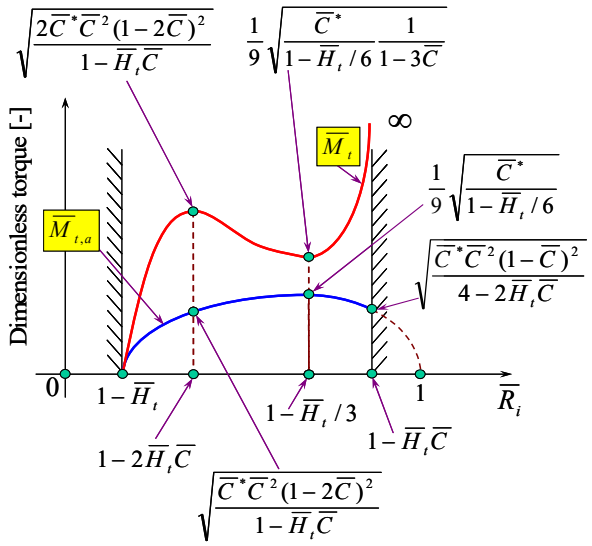

Fig. 18 Comparison of the results concerning the variation of the dimensionless torque at the shaft of the motor-generator versus the dimensionless radius of the inner rail

Fig. 19 shows, based on (41), the nonlinear descending variation of the dimensionless approximate mechanical power $\overline{P}_{mech,a}=P_{mech,a}/P_{mech,0}$ inputted at the shaft of the geared motor-generator versus the dimensionless radius $\overline{R}_i$ of the inner rail, where the referential power $P_{mech,0}$ is defined as follows:

$$P_{mech,0}=\frac{mgR_o}{2T}\overline{H}_t^2 \quad (50)$$

Thus, power $\overline{P}_{mech,a}$ displays a maximum for $\overline{R}_i=1-\overline{H}_t$, and becomes nil for $\overline{R}_i=1$.

Fig. 20 shows, based on (42), the valley-like variation of the dimensionless exact mechanical power $\overline{P}_{mech}=P_{mech}/P_{mech,0}$ inputted at the shaft of the geared motor-generator versus the dimensionless radius $\overline{R}_i$ of the inner rail. One observes that the power $\overline{P}_{mech}$ starts from a finite value at $\overline{R}_i=1-\overline{H}_t$, displays a minimum for $\overline{R}_i=1-2\overline{H}_t\overline{C}$, and then, tends to infinity for $\overline{R}_i\to 1-\overline{H}_t\overline{C}$. Again, such mechanical power distribution is obtained under the condition that the point corresponding to the minimal value of the torque ($\overline{R}_i=1-2\overline{H}_t\overline{C}$) exceeds $\overline{R}_i=1-\overline{H}_t$, i.e., under the condition $\overline{C}<1/2$. Moreover, in fact, a severer restriction ($\overline{C}<1/3$) should be imposed, as argued in the previous analysis of the torque (see (49)).

Fig. 21 compares the results separately presented by Figs. 19 and 20, concerning the dimensionless mechanical power at the shaft of the DCGMG, found by using the approximate and exact solutions. As expected, the approximate power $\overline{P}_{mech,a}$ has a different pattern of variation against the radius of the inner rail, and it is smaller than the torque $\overline{P}_{mech}$ for any $\overline{R}_i$.

Open Science Index, Energy and Power Engineering Vol:12, No:9, 2018 publications.waset.org/10009395.pdf

Open Science Index, Energy and Power Engineering Vol:12, No:9, 2018 publications.waset.org/10009395.pdf

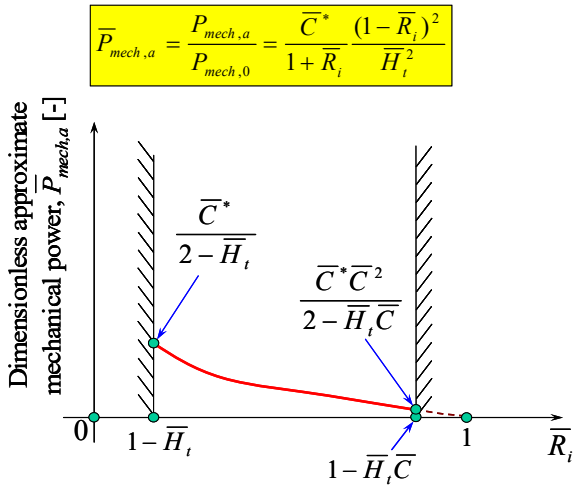

Fig. 19 Variation of the dimensionless approximate mechanical power inputted at the shaft of the motor-generator versus the dimensionless radius of the inner rail

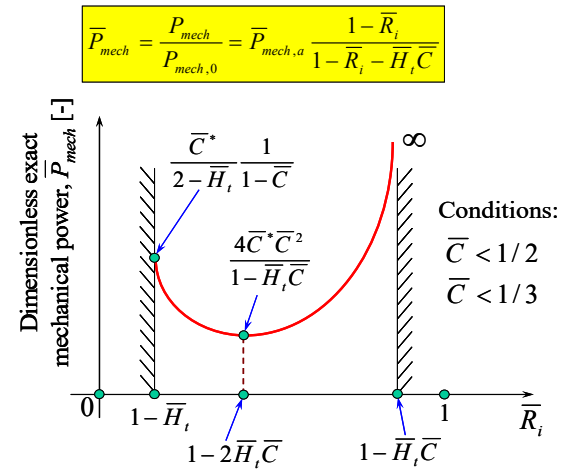

Fig. 20 Variation of the dimensionless exact mechanical power inputted at the shaft of the motor-generator versus the dimensionless radius of the inner rail

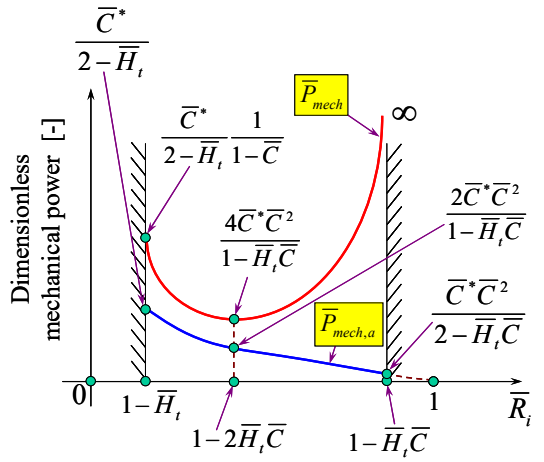

Fig. 21 Comparison of the results concerning the variation of the dimensionless mechanical power inputted at the shaft of the motor-generator versus the dimensionless radius of the inner rail

Based on (42) and Fig. 20, one discerns the influence of the various geometrical and contact parameters on the mechanical power inputted at the shaft of the DCGMG. Thus, P_{mech} varies directly proportionally to the mass m of the DCGMG, to the gravitational acceleration g, to the radius R_o of the outer rail, to the third power of the dimensionless span $1-\overline{R}_i$ of the rails, and to the sum of the sliding friction coefficients $\mu_o + \mu_i$ at the contact between the cones and the rails. On the other hand, P_{mech} varies inversely proportionally to the mean dimensionless radius $0.5(1+\overline{R}_i)$ of the rails, and to the period T of the waves (Fig. 7). Thus, the proposed water wave-powered generator is intended to mainly operate in the regime of gravitational waves induced by the wind, in the proximity of the highest peak of the power spectrum, i.e. for wave periods of $T = 8$-13 s (see Fig. 7). Moreover, analyzing the denominator of (42) in correlation with (45) and (49), which determine the allowable range of selection for the outer contact friction coefficient μ_o for a given inner contact friction coefficient μ_i, one concludes that it is desirable to provide as large as possible friction coefficient at the outer contact. In such case, augmentation of the apex angle of the cones is beneficial for the effect of power generation.

VII. Conclusions

In this work, a wave-powered electrical generator that uses a DCGMG was proposed and its output was theoretically evaluated. It appears that, in order to augment the generated electrical power, the designer has the following options:

1) To increase the mass of the DCGMG;
2) To increase the span of the rails, which can be achieved by increasing the outer radius of the rails and/or by decreasing the inner radius of the rails;
3) For a given sliding friction coefficient at the contact of the inner cone with the inner rail, to increase as much as possible the sliding friction coefficient at the contact of the outer cone with the outer rail;
4) To augment the apex angle of the cones, under limitations previously discussed in the results section;
5) To provide large amplification factor for the gear-box used in the construction of the geared motor-generator;
6) To select a motor-generator of high electro-mechanical efficiency.

References

[1] B. Drew, A. R. Plummer, and M. N. Sahinkaya, "A Review of Wave Energy Converter Technology," *Journal of Power and Energy*, 223, pp. 887–902, 2009.
[2] R. Kempener, and F. Neumann, Wave *Energy Technology*. Abu Dhabi: International Renewable Energy Agency, 2004, pp. 1–28.
[3] J. Twidell, and T. Weir, *Renewable Energy Sources*. New York: Taylor & Francis, 2006, pp. 400–429.
[4] P. Meisen, and A. Loiseau, *Ocean Energy Technologies for Renewable Energy Generation*. San Diego: Global Energy Network Institute, 2009, pp. 1–27.
[5] R. Waters, *Energy from Ocean Waves*. Uppsala University: PhD Thesis, 2008, pp. 1–132.

[6] A. S. Kumar, "Simple and Nonstop Buoyant Arm Wave Energy Converter," *International Journal of Innovative Research & Development*, 3(10), pp. 180–183, 2014.
[7] H. K. Sachs, and G. A. Sachs, "Mechanism for Generating Power from Wave Motion on a Body of Water," *US Patent*, 4,352,023, pp. 1–16, 1982.
[8] V. Orlando, "System for Generating Electrical Energy from Sea Waves," *US Patent*, 239,643, pp. 1–15, 2014.
[9] G. Bracco, E. Giorcelli, and G. Mattiazzo, "Performance Assessment of a 2DOF Gyroscopic Wave Energy Converter," *Journal of Theoretical and Applied Mechanics*, 53, pp. 195–207, 2015.
[10] H. Kanki, "Gyro Wave Activated Power Generator and a Wave Suppressor using the Power Generator," *US Patent*, 7,003,947, pp. 1–11, 2006.
[11] B. Suciu, "Solution to the Problem of Contact between a Double-Cone and Two Eccentric Circular Rails used in the Construction of a Wave-Powered Electrical Generator," *Transactions of the JSME*, 83(853), pp. 17.00093.1–12, 2017 (in Japanese).
[12] A. A. Gallitto, and E. Fiordilino, "The Double Cone: A Mechanical Paradox or a Geometrical Constraint?," *Physics Education*, 46, pp. 682–684, 2011.
[13] S. C. Gandhi, and C. J. Efthimiou, "The Ascending Double-Cone: A Closer Look at a Familiar Demonstration," *European Journal of Physics*, 26, pp. 681–697, 2005.
[14] B. Suciu, "On the Kinematics of a Double-Cone Gravitational Motor," *International Journal of Science and Engineering Investigations*, 5(53), pp. 1–7, 2016.
[15] B. Suciu, "Frictional Effects on the Dynamics of a Truncated Double-Cone Gravitational Motor, *International Journal of Mechanical, Aerospace, Industrial, Mechatronic and Manufacturing Engineering*, 11(1), pp. 28–38, 2017.
[16] N. Balta, "New Versions of the Rolling Double Cone," *Physics Teacher*, 40, pp. 156–157, 2002.
[17] H. A. Rothbart, *Mechanical Design and Systems Handbook*. New York: McGraw-Hill, 1985, pp. 7–173.
[18] R. C. Juvinall, and K. M. Marshek, *Fundamentals of Machine Component Design*. London: John Willey & Sons, 2006, pp. 1–769.
[19] J. A. Stratton, *Electromagnetic Theory*. London: McGraw-Hill, 1941, pp. 185–222.
[20] K. M. Rao, *Elements of Electrical Engineering*. New Delhi: I.K. International Publishing, 2015, pp. 1–227.
[21] A. Pramanik, *Electromagnetism*. New Delhi: PHI Learning, 2014, pp. 12–621.

Barenten Suciu was born on July 9, 1967. He received Dr. Eng. Degrees in the field of Mech. Eng. from the Polytechnic University of Bucharest, in 1997, and from the Kobe University, in 2003. He is working as Professor at the Department of Intelligent Mech. Eng., Fukuoka Institute of Technology. He is also entrusted with the function of Director of the Electronics Research Institute, affiliated to the Fukuoka Institute of Technology. He is member of JSME and JSAE. His major field of study is the tribological and dynamical design of various machine elements.

Open Science Index, Energy and Power Engineering Vol:12, No:9, 2018 publications.waset.org/10009395.pdf